Involvement of Rabphilin-3A in Cortical Granule Exocytosis in Mouse Eggs

Nobuyuki Masumoto,* Takuya Sasaki,‡ Masahiro Tahara,* Akiko Mammoto,* Yoshihide Ikebuchi,* Keiichi Tasaka,* Masahiro Tokunaga,‡ Yoshimi Takai,‡ and Akira Miyake*

*Department of Obstetrics and Gynecology, ‡Department of Molecular Biology and Biochemistry, Osaka University Medical School, Osaka 565, Japan

Abstract. Rabphilin-3A is a putative target protein for Rab3A, a member of the small GTP-binding protein superfamily that has been suggested to play a role in regulated exocytosis in presynapses. In this study we determined the expression and the function of Rabphilin-3A in mouse eggs at fertilization. Rabphilin-3A mRNA and protein were detected by reverse transcriptase–PCR and immunoblot analysis, respectively, in metaphase II mouse eggs. Immunofluorescence analysis showed that Rabphilin-3A protein was distributed in the cortical region in eggs. Sperm induces cortical granule (CG) exocytosis via an increase in cytosolic Ca^{2+} at fertilization. We microinjected the NH_2- or COOH-terminal fragment of recombinant Rabphilin-3A into metaphase II eggs. Neither treatments altered the sperm-induced cytosolic Ca^{2+} increase, but both inhibited CG exocytosis in a dose-dependent manner. The NH_2-terminal fragment was more effective than the COOH-terminal fragment. Full-length Rabphilin-3A did not affect CG exocytosis, but it attenuated the inhibition of CG exocytosis by the NH_2-terminal fragment. These results show that Rabphilin-3A is involved in Ca^{2+}-dependent CG exocytosis at fertilization in mouse eggs.

CORTICAL granule (CG)[1] exocytosis in mammalian eggs is the first important event in fertilization, which functions to block polyspermy (9, 12, 38). Sperm induces an increase in cytosolic Ca^{2+} concentration ($[Ca^{2+}]_i$) (22) that triggers the fusion of CG vesicles to the plasma membrane. It has been established that the $[Ca^{2+}]$ increase induced by sperm is essential for CG exocytosis (15, 33), but little is known about the intracellular signaling mechanism underlying this effect.

The Rab family of small GTP-binding proteins has been implicated in intracellular vesicle traffic such as exocytosis, endocytosis, and transcytosis (25, 27, 32, 34, 39). Particularly, Rab3A has been suggested to be involved in regulated exocytosis such as neurotransmitter release from presynapses (25). Recently, Rabphilin-3A, a putative target protein for Rab3A, was purified and its cDNA was sequenced (30, 31). Rabphilin-3A is a protein of 704 amino acids with a M_r of 77,976 that binds Rab3A at its NH_2-terminal region. Rabphilin-3A has two repeated C2 domains at its COOH-terminal region. This C2 region was found in protein kinase C and synaptotagmin, which are known to bind Ca^{2+} and phospholipid through this region (36). These lines of evidence indicate that Rabphilin-3A may function with Rab3A as an intracellular signal in Ca^{2+}-regulated exocytosis.

If the Rab–Rabphilin system is involved in Ca^{2+}-regulated exocytosis, the system may function in CG exocytosis in eggs at fertilization. However, to date, Rabphilin-3A expression has been reported only in neurons and neuronendocrine cells such as adrenal chromaffin and PC12 cells (11, 17, 23). There have been no reports regarding Rab or Rabphilin expression in eggs. Thus, in the present study we investigated whether Rabphilin-3A is involved in the intracellular signaling pathway responsible for CG exocytosis at fertilization in mouse eggs.

Materials and Methods

Media

M2 medium (94.7 mM NaCl, 4.78 mM KCl, 1.71 mM $CaCl_2H_2O$, 1.19 mM $MgCl_27H_2O$, 1.19 mM KH_2PO_4, 4 mM $NaHCO_3$, 21.0 mM Hepes, 5.56 mM glucose, 0.33 mM pyruvic acid, 23.3 mM sodium-lactase, 0.05 mg/ml streptomycin, 100 IU/ml penicillin G, 4 mg/ml BSA), TYH medium (119.37 mM NaCl, 4.78 mM KCl, 12.6 mM $CaCl_2H_2O$, 1.19 mM $MgCl_27H_2O$, 1.19 mM KH_2PO_4, 25.07 mM $NaHCO_3$, 5.56 mM glucose, 1 mM pyruvic acid, 0.05 mg/ml streptomycin, 75 IU/ml penicillin G, 4 mg/ml BSA), and an intracellular-like medium (ICM; 120 mM KCl, 20 mM Hepes, 100 μM EGTA, 10 mM sodium-glycerophosphate, 200 μM PMSF, 1 mM DTT) were used in these experiments. Media were made with cell culture reagents and tis-

Address all correspondence to Nobuyuki Masumoto, Department of Obstetrics and Gynecology, Osaka University Medical School, Yamadaoka, Suita, Osaka 565, Japan. Tel.: (81) 6-879-3354. Fax: (81) 6-879-3359. e-mail: masumoto@gyne.med.osaka-u.ac.jp

1. *Abbreviations used in this paper:* aa, amino acid; $[Ca^{2+}]_i$, cytosolic Ca^{2+} concentration; CG, cortical granule; GST, glutathione-*S*-transferase; HA, hemagglutinin; LCA, Lens culinaris agglutinin; RT, reverse transcriptase.

sue-culture grade water. All chemicals were obtained from Sigma Chemical Co. (St. Louis, MO) except where noted. The pH of the media was adjusted with HCl or NaOH to 7.4. All media were filtrated through 0.2-mm filters and equilibrated in an atmosphere of 5% CO_2 and 95% air at 37°C.

Preparation of Gametes

Unfertilized metaphase II eggs were collected from CD1 female mice (Charles River, Kanagawa, Japan) that were superovulated by intraperitoneal injection of 5 IU pregnant mare serum gonadotropin, followed 48 h later by 5 IU human chorionic gonadotropin. Eggs were collected from the ampulla of the oviduct 14–16 h later and placed in M2 medium covered by light mineral oil. The cumulus cells were removed by digestion (~5 min) with 0.3 mg/ml hyaluronidase (type IV-S). Only normal, mature eggs with a fully formed first polar body were used in these experiments. In some experiments, the zona pellucidae were removed by a brief exposure (~1 min) to acid Tyrode's solution (pH 2.5). The eggs were then drawn into and expelled from a small bore pipette to ensure removal of the zona pellucidae. After each procedure, the eggs were thoroughly washed in M16 medium. Eggs were cultured in petri dishes in 100-µl drops of M16 under mineral oil and incubated in an atmosphere of 5% CO_2 and 95% air at 37°C.

Spermatozoa were obtained from CD1 male mice (Charles River) of proven fertility. Spermatozoa were released from the cauda epididymis into TYH medium containing 0.3% BSA (fraction V; Sigma Chemical Co.). After incubation for 10 min in an atmosphere of 5% CO_2 and 95% air at 37°C, the sperm concentration was adjusted to 1–2 × 10^6 spermatozoa per ml. The sperm suspension was overlain with paraffin oil and further incubated for 3 h.

Purification of GST–Rabphilin-3A

Recombinant Rabphilin-3A with glutathione-S-transferase (GST) was purified as previously described (29, 36). To produce the NH_2-terminal (1–280 amino acids) and the COOH-terminal fragments (281–704 amino acids) of Rabphilin-3A, expression plasmids pGEX-2T–Rabphilin-3A-N and pGEX-2T–Rabphilin-3A-C were constructed as follows. The 0.84-kb cDNA fragment encoding the NH_2-terminal fragment and the 1.3-kilobase cDNA fragment encoding the COOH-terminal fragment with the BamHI and KpnI sites upstream of the initiator methionine codon and downstream of the termination codon were synthesized by PCR. These fragments were digested by BamHI and inserted into the BamHI site of pGEX-2T. The NH_2- and COOH-terminal fragments of Rabphilin-3A with GST were produced in *Escherichia coli* and purified by glutathione–Sepharose 4B column chromatography. Characterization of these GST fusion proteins was described in detail previously (29). GTPγS-Rab3A bound to the GST NH_2-terminal fragment of Rabphilin-3A, but did not bind to the GST C-terminal fragment; $^{45}Ca^{2+}$ bound to the GST COOH-terminal fragment of Rabphilin-3A, but did not bind to the GST NH_2-terminal fragment of Rabphilin-3A; and liposomes bound to the GST COOH-terminal fragment of Rabphilin-3A in a Ca^{2+}-dependent manner, but did not bind to the GST NH_2-terminal fragment. These samples were added to ICM solution after concentration using centricon membranes (final dose: 100 µM).

Purification of Hemagglutinin-tagged Rabphilin-3A

A DNA fragment encoding the hemagglutinin (HA) (YPYDVPDYA) epitope with the methionine codon was inserted into the BamHI site of pACYM1 *Autographa california* baculovirus transfer vector to express the HA-tagged fusion proteins (pACYM1-HA). To generate full-length (1–704 amino acids [aa], pACYM1-HA–Rabphilin-3A) and deletion mutant constructs (1–280 aa, HA–Rabphilin-3A-N; 396–704 aa, Rabphilin-3A-C) of bovine brain Rabphilin-3A, cDNAs were made by PCR using specific oligonucleotide primers inserted into pACYM1-HA and expressed as fusion proteins with the NH_2-terminal HA epitope using the insect/baculovirus system as described (2 1). Recombinant HA-tagged Rabphilin-3A was purified from the membrane fraction of overexpressing Sf9 cells by the same methods as those used for Rabphilin-3A without HA (29). HA-tagged Rabphilin-3A expressed endogenously in cells is known to function in Ca^{2+}-regulated exocytosis (3, 16).

Generation of Rabphilin-3A Polyclonal Antibodies

Rabbit antisera were raised against the GST-binding NH_2-terminal fragment and the COOH-terminal fragment of Rabphilin-3A (36). The anti-

Rabphilin-3A monospecific antibodies were purified from the antisera by affinity column chromatography using the same protein fragments as ligands. Immunofluorescence and immunoblot analyses were carried out using these antibodies.

mRNA Extraction and Reverse Transcriptase–PCR

Metaphase II–arrested eggs were collected, immediately frozen in a liquid nitrogen, and stored at −80°C until mRNA extraction by oligo(dT)-cellulose (Micro mRNA Purification Kit; Pharmacia Biotech, Piscataway, NJ). The mRNA isolated from the eggs was then reverse transcribed into cDNA. The Rabphilin-3A oligonucleotides primers were synthesized on a DNA/RNA synthesizer (model 394; Applied Biosystems, Foster City, CA). The primer sequences and their corresponding locations in the nucleotide sequence of mouse Rabphilin-3A (11) were as follows: Rabphilin-3A–primer1, forward: 5'-GCAGAGAAGATGGAAGCCATG-3' (181–201); reverse: 5'-CCACACTTGGTGCAGACATTC-3' (348–368); Rabphilin-primer2, forward: 5'-GGAGGAGGAAGAAGCCAATAG-3' (1092–1112); reverse: 5'-AGGCAGCAGATGAAGCTTCAC-3' (1255–1275). These sequence data are available under EMBL/GenBank/DDBJ accession number D29965.

Rabphilin-3A cDNAs were amplified singly. The PCR mixtures of Rabphilin-3A cDNA and respective primers were amplified using a program temperature control system (PC-700; Astec Co., Fukuoka, Japan). One cycle of PCR consisted of 30 s at 94°C, 60 s at 58°C, and 30 s at 72°C; a total of 35 cycles was performed. Mouse brain RNA samples were used as positive controls for Rabphilin-3A. These RNA samples were also amplified without reverse transcription as negative controls. Each PCR reaction mixture was subjected to 2% agarose gel electrophoresis, and the amplified products were visualized by staining with ethidium bromide for 30 min at room temperature.

To confirm the specificity of PCR, amplified cDNAs were digested by each restriction enzyme, and the digests were analyzed by 4.8% PAGE and stained with ethidium bromide. The bands were also identified by reverse transcriptase (RT)–PCR Southern blot analysis. Analysis consisted of the following steps. Fractionated DNA was transferred onto a nitrocellulose filter, and the filter was hybridized with ^{32}P-multiprime (Amersham Corp., Arlington Heights, IL)–labeled Rabphilin-3A cDNA probes. The filter was washed under high stringency conditions and exposed overnight to XAR-5 film (Eastman Kodak Co., Rochester, NY).

Immunoblot Analysis

About 500 eggs were collected in PBS (pH 7.4) containing 3 mg/ml of polyvinyl pyrrolidone and were solubilized by lysis buffer composed of 15% SDS. As positive controls for Rabphilin-3A, mouse brain and purified bovine Rabphilin-3A were prepared. Lysed samples were concentrated with microcon, and SDS-PAGE was performed using a microslab gel (30 × 30 × 1 mm). Samples were run through the stacking gel and separating gel at 10 mA per gel. The proteins were electrophoretically transferred onto a nitrocellulose membrane sheet, and the transferred proteins were immunoblotted using a polyclonal antibody against the NH_2-terminal fragment of Rabphilin-3A. Biotinylated anti–rabbit IgG (goat, 1:4,000) was used as a secondary antibody. Finally, avidin-conjugated alkaline phosphatase was applied, and the filter was stained with 5-bromo-4-chloro-3-indoyl-phosphate/nitroblue tetrazolium (BCIP/NBT; Bio Rad Laboratories, Richmond, CA).

Immunofluorescence

The metaphase II–arrested eggs were rinsed and fixed with Zamboni's fixative (0.2% picric acid and 2% paraformaldehyde). Rabbit polyclonal antibodies against the NH_2- and COOH-terminal fragments of Rabphilin-3A were applied as primary antibodies for 24 h at 4°C. Negative control experiments for each antibody included replacement of the primary antibody with nonimmune rabbit IgG at the same concentration. After repeated washing in PBS, biotinylated anti–rabbit IgG (goat, 1:1,000) was applied for 24 h at 4°C. After repeated washing in PBS, avidin-FITC was applied for 30 min at 37°C. Unbound antibody was rinsed off, and the fluorescence of FITC was visualized by excitation at 488 nm with the argon laser in the confocal laser microscope. The confocal parameters of scan rate, aperture, gain, black level, and frames accumulated were the same for all samples.

Microinjection

Samples (10 pl, 5–100 μM, GST-bound or HA-tagged Rabphilin-3A) were microinjected into the cytoplasm of eggs using micromanipulators and a microinjector (Eppendorf, Tokyo, Japan). A fire-polished holding pipette and a beveled injection pipette with an outer 3-μm diam was used. Injected eggs were used in $[Ca^{2+}]_i$ and CG exocytosis experiments after a 30-min incubation in M16 medium.

Measurement of $[Ca^{2+}]_i$

$[Ca^{2+}]_i$ was monitored with a digital imaging fluorescence microscope using the Ca^{2+}-sensitive fluorescent dye, fura-2-AM (18, 33). Eggs were incubated at 37°C for 60 min in M16 medium containing 5 μM fura-2-AM (Wako Pure Chemical Industries, Ltd., Tokyo, Japan). The eggs were then rinsed with TYH medium and placed on the microscope stage. The $[Ca^{2+}]_i$ of eggs was measured at 7.5-s intervals with a digital imaging microscopic system (Mu-1000; Scholar Tec Corp., Osaka, Japan). $[Ca^{2+}]_i$ was calculated by the ratio of the intensities of fluorescent emission at 510 nm with excitation at 340 and 380 nm. The fluorescent excitation beam was targeted on the cells, and then the emission fluorescence was recorded with a digital imaging analysis and a computer.

Measurement of Exocytosis in Living Eggs

As previously described (33), exocytosis in living eggs was measured using the membrane-impermeable membrane probe TMA-DPH (Molecular Probes, Eugene, OR). Zona-free eggs were plated in a 90-μl drop of TYH medium on glass coverslips that were sealed under a 1.0-cm hole in the bottom of 35-mm culture dishes and coated with poly-L-lysine. Drops of TYH medium containing eggs were overlain with oil, and 10 μl of 50 μM TMA-DPH was added into the drop at 37°C, to a final concentration of 5 μM. The 430-nm emission fluorescence of single eggs at 350-nm excitation was measured, and changes in the fluorescence intensity in individual eggs were analyzed with a digital imaging microscopy system (Mu-1000; Scholar Tec Corp.). Eggs were inseminated with spermatozoa, the final concentration of which was 1–2 × 10⁵ spermatozoa per ml. After a spermatozoan attached to the plasma membrane of a zona-free egg, the 430-nm fluorescence of the egg at 350-nm excitation was measured. The percentage increase of fluorescence was represented as the total of exocytosis. Eggs were intermittently irradiated for 50 ms every 15 s to prevent UV damage.

Labeling of CGs with Lens Culinaris Agglutinin

Exocytosis of CGs was evaluated by Lens culinaris agglutinin (LCA) staining (2, 4). 30–40 min after fertilization, unfixed eggs were washed in M16 medium and incubated for 15 min in 10 μg/ml FITC-conjugated LCA (E-Y Laboratories, San Mateo, CA). These eggs were washed (five times, 5 min each) before examination by laser scanning confocal microscopy 2 h after fertilization. The CG exudate remained on the surface of the activated eggs after fertilization. The eggs were excited at 488 nm by the argon laser in the confocal laser microscope, and confocal optical images of FITC-LCA were analyzed. The confocal parameters of scan rate, aperture, gain, black level, and frames accumulated were the same for all samples. In control experiments, eggs were exposed to FITC-LCA in 100 mM α-methylmannoside for 10 min before incubation.

Data Analysis and Statistics

All experiments were repeated more than four times, and representative results are shown. The data shown in Fig. 6, b and c, are expressed as means + SD of multiple determinations from the data of 30 eggs. The homoscedasticity of the data was analyzed by Bartlett's test. The significance of differences was assessed by analysis of variance, followed by Scheffe's multiple comparison, and a P value of <0.01 was taken to be significant.

Results

Expression of Rabphilin-3A mRNA in Metaphase II Eggs

RT-PCR was performed to detect Rabphilin-3A gene transcripts in unfertilized eggs. cDNA samples reverse tran-

scribed from mRNA isolated from eggs were amplified using the two groups of synthesized Rabphilin-3A primers. Two amplified products of 188 and 181 bp were observed in Fig. 1, showing that Rabphilin-3A mRNA was expressed in metaphase II eggs. No amplified DNA fragments were observed when PCR was performed without prior reverse transcription (Fig. 1). This shows that the amplified fragments were generated from Rabphilin-3A mRNA and did not originate from genomic DNA. The specificity of the respective bands was determined by digesting the PCR products with restriction enzymes. The first fragment (188 bp) was separated to 121- and 67-bp fragments by ALV2 (Fig. 1). The second fragment (181 bp) was separated to 124- and 57-bp fragments by EcoRI (Fig. 1). Moreover, the sequences of 188- and 181-bp fragments were confirmed by Southern blot analysis and direct sequencing (not shown).

### Presence of Rabphilin-3A Protein in Metaphase II Eggs

We determined the presence of Rabphilin-3A protein in metaphase II eggs by immunoblot analysis. A 78-kD band was specifically labeled with antibody against NH₂-terminal of Rabphilin-3A (Fig. 2). As positive controls, similar bands were identified in mouse brain and bovine Rabphilin-3A protein (Fig. 2).

Distribution of Rabphilin-3A Protein in Metaphase II Eggs

Intracellular distribution of Rabphilin protein in metaphase II eggs was determined by immunofluorescence methods using a confocal microscope. Specific staining labeling with antibodies against the NH₂- and COOH-terminal fragments of Rabphilin-3A was observed in eggs (Fig. 3). When primary antibodies were substituted with
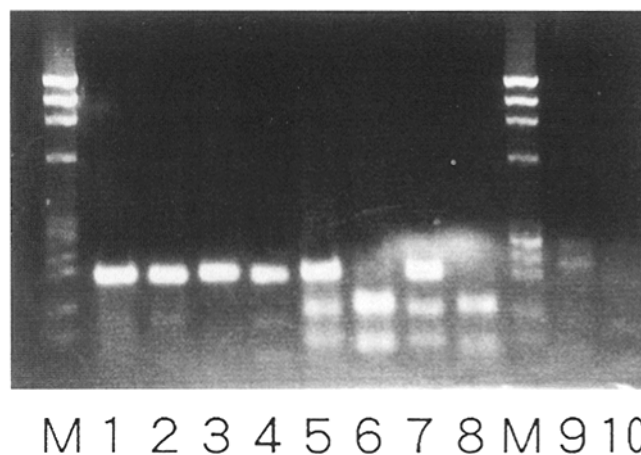

Figure 1. Ethidium bromide staining of RT-PCR products using two sets of Rabphilin-3A primers in metaphase II eggs and brain. DNA size marker ∅X174 (*M*); mouse eggs (lanes *1* and *2*); mouse brain (lanes *3* and *4*), PCR products from lanes *1* and *2* digested by restriction enzyme (lanes *5* and *6*); PCR products from lane *3* and *4* digested by restriction enzyme (lanes *7* and *8*); samples from lanes *1* and *2* amplified without RT as negative controls (lanes *9* and *10*). Lanes *1*, *3*, *5*, *7*, and *9* and lanes *2*, *4*, *6*, *8*, and *10* were amplified using the same primers, respectively.
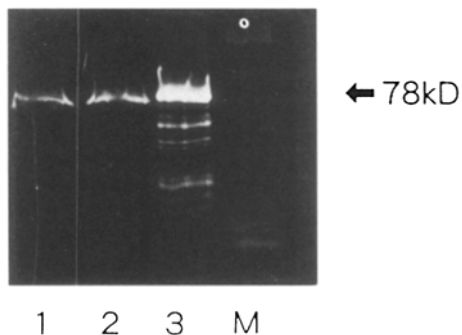
Figure 2. Immunoblot analysis of Rabphilin-3A. The polyclonal antibody against the NH_2-terminal fragment of Rabphilin-3A was used as a primary antibody. Molecular weight marker (M); mouse eggs (lane 1); mouse brain (lane 2); bovine Rabphilin-3A (lane 3).

nonimmune rabbit IgG, no specific staining was observed (Fig. 3). Staining for both fragments was distributed in the cortical region in eggs. The staining intensity was not homogeneous. In some eggs, a staining-free region near the inside of the plasma membrane was observed.
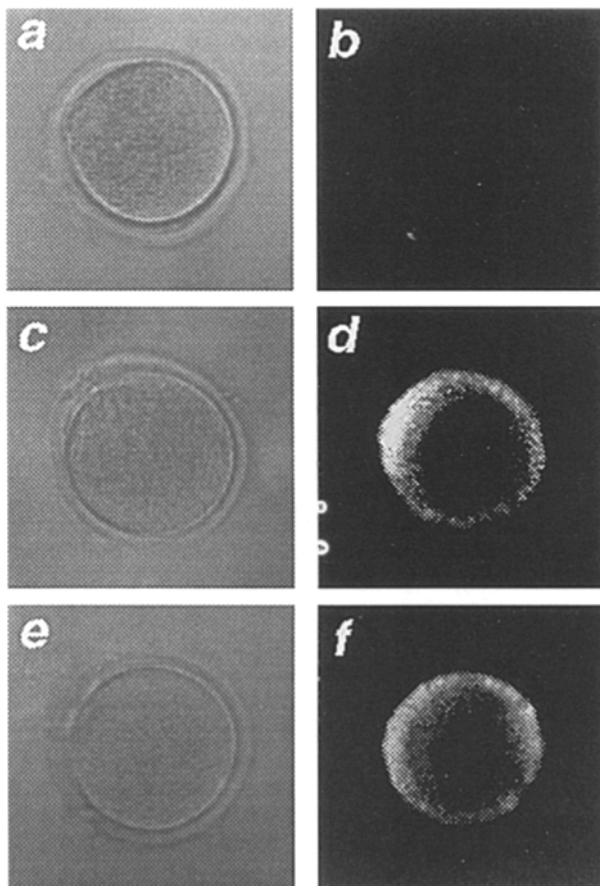
Figure 3. Confocal optical images of Rabphilin-3A immunofluorescence in metaphase II eggs. Nonimmune rabbit IgG (b), polyclonal antibody against the NH_2-terminal fragment of Rabphilin-3A (d), and polyclonal antibody against the COOH-terminal fragment of Rabphilin-3A (f) were used as primary antibodies, respectively. Phase-contrast images (a, c, and e) corresponded to fluorescence images (b, d, and f), respectively.

Effects of the GST NH_2- or COOH-terminal Rabphilin-3A Fragments on $[Ca^{2+}]_i$ and the Surface Area Increase due to Exocytosis

To determine the function of Rabphilin-3A in the egg at fertilization, the GST-bound NH_2- or COOH-terminal fragments of Rabphilin-3A, or GST as a control, were microinjected into the egg cytoplasm. Then, the zona pellucidae of the treated eggs were removed, and the zona-free eggs were inseminated by spermatozoa. Exocytosis was evaluated by membrane surface area using the membrane dye TMA-DPH. In control eggs, repetitive increases in $[Ca^{2+}]_i$ and exocytosis were observed (Fig. 4). In eggs treated with the intracellular Ca^{2+} chelator BAPTA-AM as a negative control, both the increases in $[Ca^{2+}]_i$ and exocytosis were blocked (Fig. 4). Exocytosis at fertilization was blocked in respective eggs injected with the NH_2- or COOH-terminal fragments of Rabphilin-3A, but not in those injected with only GST (Fig. 4). The $[Ca^{2+}]_i$ changes in these three groups of eggs were not inhibited (Fig. 4). These results indicate that the NH_2- or COOH-terminal fragment of Rabphilin-3A specifically blocked a pathway downstream of Ca^{2+} mobilization.

Effects of the GST NH_2- or COOH-terminal Rabphilin-3A Fragments on the Release of CG Contents

Release of CG content was evaluated by LCA staining as another assay for CG exocytosis. FITC-LCA fluorescence was observed around the plasma membrane in inseminated eggs. This fluorescence represented CG exudate, and CG secretion was induced by sperm in almost all of the eggs at fertilization under the conditions used here. A GST-bound NH_2- or COOH-terminal fragment of Rabphilin-3A, or GST as a control, was injected into the egg cytoplasm, the treated eggs were inseminated by sperm, and optical images of LCA fluorescence were observed using a confocal laser microscope (Fig. 5 a). Intensities of LCA fluorescence in eggs were analyzed in respective groups. The increase of LCA fluorescence induced by fertilization was dose dependently inhibited by microinjection of the GST-bound NH_2- or COOH-terminal fragment of Rabphilin-3A (Fig. 5 b). The GST-bound NH_2-terminal fragment of Rabphilin-3A showed almost complete inhibition at concentrations in excess of 10 μM. The GST-bound COOH-terminal fragment of Rabphilin-3A showed almost complete inhibition at >40 μM. Injection of GST (100 μM) alone did not affect the release of CG contents (not shown).

Effects of the HA-tagged Full-Length, NH_2- or COOH-terminal Rabphilin-3A on the Release of CG Contents

Next, HA-tagged NH_2- or COOH-terminal fragments or full-length Rabphilin-3A were injected at the respective effective concentration. The increase of LCA fluorescence induced by fertilization was significantly inhibited by microinjection of the HA-tagged NH_2-terminal (10 μM) or COOH-terminal fragment (40 μM), but not by the full-length Rabphilin-3A (20 μM) (Fig. 5 c). The inhibition by the HA-tagged NH_2-terminal fragment of Rabphilin-3A
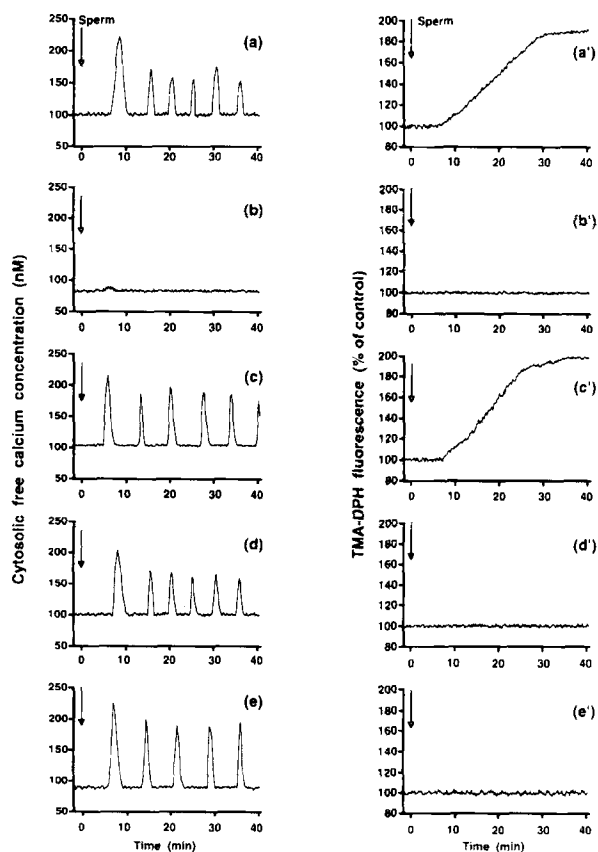
Figure 4. $[Ca^{2+}]_i$ change and exocytosis at fertilization in eggs (*a* and *a'*); eggs treated with 10 μM BAPTA-AM (*b* and *b'*); eggs microinjected with only GST (*c* and *c'*); GST-bound NH_2-terminal fragment (*d* and *d'*); and GST-bound COOH-terminal fragment (*e* and *e'*) of Rabphilin-3A. Increases in TMA-DPH fluorescence represent exocytosis.

(10 μM) was partially attenuated by the full-length molecule (20 μM). These results indicate that nonfunctional mutant fragments of Rabphilin-3A blocked the intracellular signal transduction pathway responsible for CG secretion by competing with intracellular native Rabphilin-3A.

Discussion

In mouse eggs, maternal mRNAs, which are degraded at the two-cell stage, support meiosis, fertilization, and the first cleavage (1, 6, 28). We demonstrated the expression of Rabphilin-3A mRNA in metaphase II eggs by RT-PCR, and our results suggest that Rabphilin-3A may play an important role in fertilization. Moreover, we determined the presence and the localization of Rabphilin-3A protein in metaphase II eggs by immunoblot analysis and immunofluorescence analysis. Rabphilin-3A is known to be localized in synaptic vesicles in neurons (23). In eggs, Rabphilin-3A was distributed in the cortical region, corresponding to the distribution pattern of CG vesicles. Moreover, the distribution of Rabphilin-3A was heterogeneous in some eggs with the presence of a Rabphilin-3A–free area in the cortical region. It has been reported that the metaphase II mouse eggs have CG-free domains that are formed during egg maturation (5, 26). However, it is not yet clear

whether Rabphilin-3A is specifically localized in CG vesicles or whether the Rabphilin-3A–free region corresponds to the CG-free region.

Next, we measured the sperm-induced $[Ca^{2+}]_i$ mobilization and exocytosis in eggs after microinjection of deletion mutant proteins to determine the function of Rabphilin-3A. We used two assays for CG exocytosis in mouse eggs at fertilization, the change of plasma membrane areas and CG exudate using the membrane-labeling dye TMA-DPH and CG-labeling dye LCA, respectively. We have established the former method to measure dynamics of exocytosis in living mouse eggs (33) or in pituitary gonadotropes (19, 20). Two different types of Rabphilin-3A mutant proteins (GST fusion protein and HA-tagged protein) were used. We confirmed that these proteins have functions endogenously and in vitro as previously described (16, 29).

Rab3A is known to be involved specifically in Ca^{2+}-regulated exocytosis in presynapses (25). Rabphilin-3A has at least two functionally different domains, the NH_2-terminal Rab3A-binding domain and the COOH-terminal two C2-like domains interacting with Ca^{2+} and phospholipid (36), and is phosphorylated by Ca^{2+}/calmodulin (7, 13). These observations suggest that Rabphilin-3A may function with Rab3A in Ca^{2+}-regulated exocytosis. It was recently reported that Rabphilin-3A is a positive regulator of exocytosis in chromaffin (3) and PC12 cells (16). We also attempted to determine the role of Rabphilin-3A in CG exocytosis at fertilization. The COOH-terminal fragment of Rabphilin-3A can bind cytosolic Ca^{2+} and phospholipid, and the NH_2-terminal fragment can bind Rab3A (29, 36). In this study, microinjection of the COOH- or the NH_2-terminal fragment of recombinant Rabphilin-3A into cytoplasm of eggs dose dependently blocked sperm-induced CG exocytosis. The NH_2-terminal fragment was effective at a lower concentration than the COOH-terminal fragment. To competitively inhibit binding to the mobilized Ca^{2+}, a higher concentration of COOH-terminal fragment may be required. Moreover, the inhibition by the NH_2-terminal fragment of Rabphilin-3A was partially attenuated by the full-length molecule. These results indicate that NH_2- or COOH-terminal fragments of Rabphilin-3A blocked CG exocytosis by competing with intracellular native Rabphilin-3A. The full-length Rabphilin-3A did not affect CG release, because CG release at fertilization may be the maximal response. Our results suggest that Rabphilin-3A functions as a Ca^{2+} sensor in Ca^{2+}-dependent CG exocytosis and communicates the sperm-induced signal to Rab3A.

The small GTP-binding proteins, Raf/Ras, were reported to be involved in mouse embryo development through the two-cell stage (37). The Rho family may also be involved in egg cleavage in *Xenopus* (14) and mouse (24). However, there have been no reports concerning the roles of small GTP-binding proteins in egg at fertilization. Rab3A, 3B, 3C, and 3D have been suggested to have roles in exocytosis. We also investigated the expression of Rab3 family mRNA in mouse metaphase II eggs. Rab3A and Rab3D, but not Rab3B or Rab3C, mRNA were expressed in mouse metaphase II eggs (manuscript submitted for publication). Rabphilin-3A was first purified from bovine brain as a putative binding protein of Rab3A (30). Recently, Rabphilin-3A was reported to bind not only

(a)

(b)

(c)
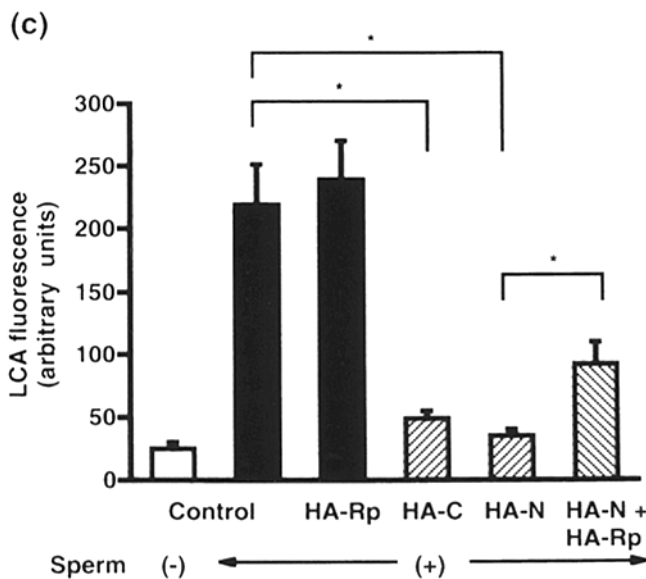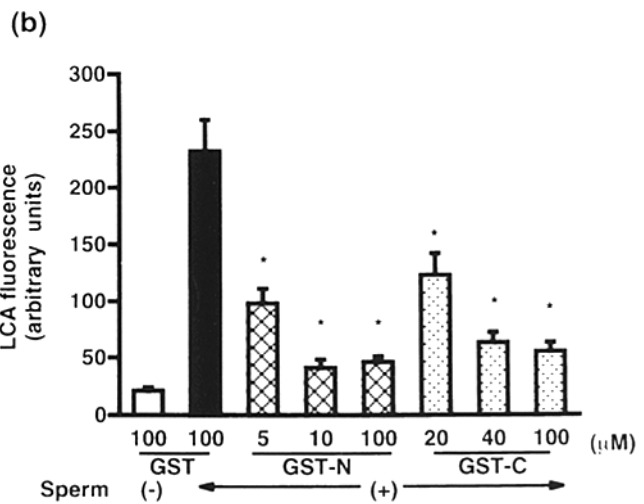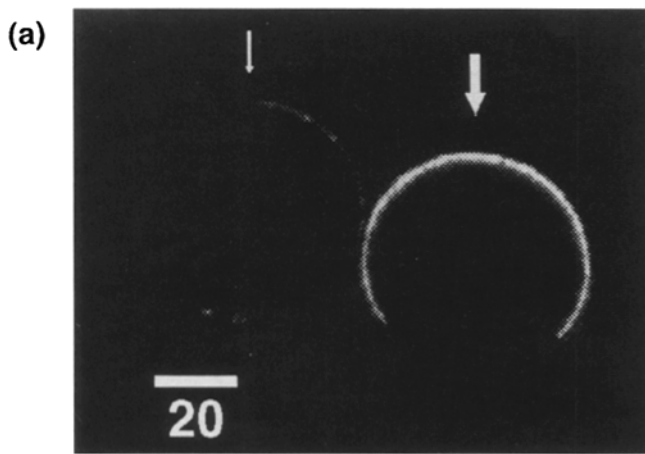
Figure 5. (*a*) Confocal optical images of LCA-FITC. Wide and narrow arrows indicate eggs microinjected with only GST (100 μM) and GST-bound NH₂-terminal fragment of Rabphilin-3A (100 μM), respectively. Microinjected eggs were stained with LCA-FITC after insemination. LCA staining shows the CG contents released from the egg. (*b*) The intensity of total LCA fluorescence in the egg after insemination. Only the GST, the GST NH₂-terminal fragment, and the GST COOH-terminal fragment of Rabphilin-3A at various concentrations were microinjected into the eggs. (*c*) The intensity of total LCA fluorescence in the egg after insemination. The HA-tagged NH₂-terminal fragment (10 μM), HA-tagged COOH-terminal fragment (40 μM), the full-length (20 μM) or HA-tagged NH₂-terminal fragment (10 μM), and full-length (20 μM) Rabphilin-3A were microinjected into the eggs.

Rab3A but also Rab3B (35) and Rab3C (17). However, it is not clear whether Rabphilin-3A binds to Rab3D. In mouse eggs, Rabphilin-3A may function by binding to Rab3A or to Rab3D. Rab3D may also function through other intracellular signaling pathways in CG exocytosis. A mouse strain with a knockout mutation of Rab3A shows normal fertility (8). In the Rab3A-knockout mouse, Rab3D may function in CG exocytosis instead of Rab3A. On the other hand, while CG exocytosis causes the zona block to polyspermy, the plasma membrane block to polyspermy, which is not dependent on CG exocytosis, is present in mouse eggs (10). Thus, the membrane block may supplement the lack of the zona block in Rab3A-knockout mouse.

In conclusion, our results indicate that the Rab–Rabphilin system is involved in the signal transduction pathway downstream of the sperm-induced intracellular Ca^{2+} mobilization.

References

1. Braude, P., H. Pelham, G. Flach, and R. Lobatto. 1979. Posttranscriptional control in the early mouse embryo. *Nature (Lond.).* 282:102–105.

2. Cherr, G., E. Drobnis, and D. Katz. 1988. Localization of cortical granule constituents before and after exocytosis in the hamster eggs. *J. Exp. Zool.* 246:81–93.

3. Chung, S., Y. Takai, and R.W. Holz. 1995. Evidence of that the Rab3a-binding protein, Rabphilin3a, enhances regulated secretion. *J. Biol. Chem.* 270:16714–16718.

4. Ducibella, T., E. Anderson, D.F. Albertini, J. Aalberg, and S. Rangarajan. 1988. Quantitative studies of chages in cortical granule number and distribution in the mouse oocyte during meiotic maturation. *Dev. Biol.* 130:184–197.

5. Ducibella, T., S. Kurasawa, S. Rangarajan, G.S. Kopf, and R.M. Schultz. 1990. Precocious loss of cortical granules during mouse oocyte meiotic maturation and correlation with an egg-induced modification of the zona pellucida. *Dev. Biol.* 137:46–55.

6. Flach, G., M.H. Johnson, P.R. Braude, R.A.S. Taylor, and V.N. Bolton. 1982. The transition from maternal to embryonic control in the 2-cell mouse embryo. *EMBO (Eur. Mol. Biol. Organ.) J.* 1:681–686.

7. Fykse, E.M., C. Li, and T.C. Sudhof. 1995. Phosphorylation of rabphilin-3A by Ca^{2+}/calmodulin- and cAMP-dependent protein kinases in vitro. *J. Neurosci.* 15:2385–2395.

8. Geppert, M., V.Y. Bolshakov, S.A. Siegelbaum, K. Takei, P. De Camilli, R.E. Hammer, and T.C. Sudhof. 1994. The role of Rab3A in neurotransmitter release. *Nature (Lond.).* 369:493–497.

9. Gulyas, B. 1980. Cortical granules of mammalian eggs. *Int. Rev. Cytol.* 63:357–392.

10. Horvath, P.M., T. Kellom, J. Caulfield, and J. Boldt. 1993. Mechanistic studies of the plasma membrane block to polyspermy in mouse eggs. *Mol. Reprod. Dev.* 34:65–72.

11. Inagaki, N., M. Mizuta, and S. Seino. 1994. Cloning of a mouse rabphilin-3A expressed in hormone-secreting cells. *J. Biochem. (Tokyo)* 116:239–242.

12. Jaffe, L., and M. Gould. 1985. Polyspermy-preventing mechanisms. *In* Biology of Fertilization. C.B. Metz and A. Monroy, editors. Academic Press, New York. 223–250.

13. Kato, M., T. Sasaki, K. Imazumi, K. Takahashi, K. Araki, H. Shirataki, Y. Matsuura, A. Ishida, H. Fujisawa, and Y. Takai. 1994. Phosphorylation of Rabphilin-3A by calmodulin-dependent protein kinase II. *Biochem. Biophys. Res. Commun.* 205:1776–1784.
14. Kishi, K., T. Sasaki, S. Kuroda, T. Itoh, and Y. Takai. 1993. Regulation of cytoplasmic division of *Xenopus* embryo by *rho* p21 and its inhibitory GDP/GTP exchange protein (*rho* GDI). *J. Cell Biol.* 120:1187–1195.
15. Kline, D., and J. Kline. 1992. Repetitive calcium transients and the role of calcium in exocytosis and cell cycle activation in the mouse egg. *Dev. Biol.* 149:80–89.
16. Komuro, R., T. Sasaki, S. Orita, M. Maeda, and Y. Takai. 1996. Involvement of Rabphilin-3A in Ca^{2+}-dependent exocytosis from PC12 cells. *Biochem. Biophys. Res. Commun.* 219:435–440.
17. Li, C., K. Takei, M. Geppert, L. Daniell, K. Stenius, E.R. Chapman, R. Jahn, P.D. Camilli, and T.C. Sudhof. 1994. Synaptic targeting of rabphilin-3A, a synaptic vesicle Ca^{2+}/phospholipid-binding protein, depends on rab3A/3C. *Neuron.* 13:885–898.
18. Masumoto, N., K. Tasaka, K. Kasahara, A. Miyake, and O. Tanizawa. 1991. Purification of gonadotropes and intracellular free calcium oscillation. Effects of gonadotropin-releasing hormone and interleukin 6. *J. Biol. Chem.* 266:6485–6488.
19. Masumoto, N., K. Tasaka, J. Mizuki, M. Tahara, A. Miyake, and O. Tanizawa. 1993. Dynamics of exocytosis, endocytosis and recycling in single pituitary gonadotropes. *Biochem. Biophys. Res. Commun.* 197:207–213.
20. Masumoto, N., K. Tasaka, J. Mizuki, K. Fukami, Y. Ikebuchi, and A. Miyake. 1995. Simultaneous measurements of exocytosis and intracellular calcium concentration with fluorescent indicators in single pituitary gonadotropes. *Cell Calcium.* 18:223–231.
21. Matsuura, Y., R.D. Possee, H.A. Overton, and D.H. Bishop. 1987. Baculovirus expression vectors: the requirements for high level expression of proteins, including glycoproteins. *J. Gen. Virol.* 68:1233–1250.
22. Miyazaki, S., N. Hashimoto, Y. Yoshimoto, T. Kishimoto, Y. Igusa, and Y. Hiramoto. 1986. Temporal and spatial dynamics of the periodic increase in intracellular free calcium at fertilization of golden hamster eggs. *Dev. Biol.* 118:259–267.
23. Mizoguchi, A., Y. Yano, H. Hamaguchi, H. Yanagida, C. Ide, A. Zahraoui, H. Shirataki, T. Sasaki, and Y. Takai. 1994. Localization of rabphilin-3A on the synaptic vesicle. *Biochem. Biophys. Res. Commun.* 202:1235–1243.
24. Moore, G.D., T. Ayabe, P.E. Visconti, R.M. Schultz, and G.S. Kopf. 1994. Roles of heterotrimeric and monomeric G proteins in sperm-induced activation of mouse eggs. *Development (Camb.).* 120:3313–3323.

25. Nuoffer, C., and W.E. Balch. 1994. GTPases: multifunctional molecular switches regulating vesicular traffic. *Annu. Rev. Biochem.* 63:949–990.
26. Okada, A., K. Inomata, and T. Nagase. 1993. Spontaneous cortical granule release and alteration of zona pellucida properties during and after meiotic maturation of mouse oocytes. *Anat. Rec.* 237:518–526.
27. Pfeffer, S.R. 1992. GTP-binding proteins in intracellular transport. *Trends Cell Biol.* 21:41–46.
28. Pratt, H.P.M., V.N. Bolton, and K.A. Gudgeon. 1983. The legacy from the oocyte and its role in controlling early development of the mouse embryo. *Ciba Found. Symp.* 98:197–227.
29. Shirataki, H., and Y. Takai. 1995. Purification and properties of rabphilin-3A. *Methods Enzymol.* 257:291–302.
30. Shirataki, H., K. Kaibuchi, K. Yamaguchi, K. Wada, H. Horiuchi, and Y. Takai. 1992. A possible target protein for *smg*-25A/*rab*3A small GTP-binding protein. *J. Biol. Chem.* 267:10946–10949.
31. Shirataki, H., K. Kaibuchi, T. Sakoda, S. Kishida, T. Yamaguchi, K. Wada, M. Miyazaki, and Y. Takai. 1993. Rabphilin-3A, a putative target protein for smg p25A/rab3A p25 small GTP-binding protein related to synaptotagmin. *Mol. Cell. Biol.* 13:2061–2068.
32. Simons, K., and M. Zerial. 1993. Rab proteins and the road maps for intracellular transport. *Neuron.* 11:789–799.
33. Tahara, M., K. Tasaka, N. Masumoto, A. Mammoto, Y. Ikebuchi, and A. Miyake. 1996. Dynamics of cortical granule exocytosis at fertilization in living mouse eggs. *Am. J. Physiol.* 270:C1354–C1361.
34. Takai, Y., K. Kaibuchi, A. Kikuchi, and M. Kawata. 1992. Small GTP-binding proteins. *Int. Rev. Cytol.* 133:187–230.
35. Weber, E., T. Jilling, and K.L. Kirk. 1996. Distinct functional properties of Rab3A and Rab3B in PC12 neuroendocrine cells. *J. Biol. Chem.* 271:6963–6971.
36. Yamaguchi, T., H. Shirataki, S. Kishida, M. Miyazaki, J. Nishikawa, K. Wada, S. Numata, K. Kaibuchi, and Y. Takai. 1993. Two functionally different domains of rabphilin-3A, rab3A p25/smg p25A-binding and phospholipid- and Ca^{2+}-binding domains. *J. Biol. Chem.* 268:27164–27170.
37. Yamauchi, N., A.A. Kiessling, and G.M. Cooper. 1994. The Ras/Raf signaling pathway is required for progression of mouse embryos through the two-cell stage. *Mol. Cell. Biol.* 14:6655–6662.
38. Yanagimachi, R. 1977. Specificity of sperm–egg interactions. *In* Immunobiology of Gametes. M. Edidin and M.H. Johnson, editors. Cambridge University Press, London. 255–295.
39. Zerial, M., and H. Stenmark. 1993. Rab GTPases in vesicular transport. *Curr. Opin. Cell Biol.* 5:613–620.